



## OPEN EXO1 is a key gene for lung-resident memory T cells and has diagnostic and predictive values for lung adenocarcinoma

Zhuoqi Li<sup>1,6</sup>, Xiaoyan Lin<sup>2,3,6</sup>, Yuanhui Yang<sup>2,6</sup>, Mei Tian<sup>4</sup>, Lu Zhang<sup>1</sup>, Fujing Huang<sup>1</sup>, Xiao Wen<sup>1</sup>, Zhigang Wei<sup>5</sup>✉ & Yuan Tian<sup>1</sup>✉

Lung adenocarcinoma (LUAD) is a very common and lethal kind of lung malignancy. An increasing number of studies indicated that tissue-resident memory T ( $T_{RM}$ ) cells played significant roles in anti-cancer immunity. In our previous study, EXO1 was found to be a core gene for  $T_{RM}$  cells in the prognosis of LUAD. However, the roles of EXO1 in the tumor microenvironment, and its application in the diagnosis and prognosis prediction of LUAD are still inadequately explored. In this study, the RNA expression, DNA methylation, CNV, somatic mutation data of EXO1, and the corresponding patients' clinical information from publicly available databases were analyzed using bioinformatic methods. The results were validated through immunohistochemical staining of EXO1 in LUAD samples. The results showed EXO1 was aberrantly highly expressed in LUAD tissues. High expression of EXO1 was a risky factor for LUAD patients. The expression level of EXO1 was associated with many clinical features such as TNM stages. It can also distinguish normal tissues and LUAD tumor tissues accurately. EXO1 expression was correlated with the infiltration of immune cells, and high expression of EXO1 was an adverse effect on LUAD patients receiving anti-PD-1/PD-L1 immunotherapy. Moreover, patients with EXO1 mutation had worse DSS, DFI and PFI.

**Keywords** EXO1, Prognosis, Diagnosis, LUAD, Risky factor, Biomarker

Lung cancer is one of the cancers with the highest morbidity, resulting in the most cancer-related deaths in the world<sup>1</sup>. Lung adenocarcinoma (LUAD) is a kind of non-small cell lung cancer (NSCLC). It is the most common lung malignancy and is usually accompanied with genetic and morphologic diversity, which caused difficulties for the diagnosis and treatment of LUAD<sup>2,3</sup>. Currently, the 5-year survival rate of LUAD patients still remains 23% despite improvements in early diagnosis and individualized treatment, and uncovering novel molecular biomarkers to establish novel diagnostic and treatment models is essential for reducing LUAD impairment<sup>4</sup>.

EXO1 (Exonuclease 1) is a 5'→3' exonuclease and 5'-flap structure-specific nuclease that belongs to the RAD2 nuclease enzymes family<sup>5,6</sup>. It can catalyze the excision of single nucleotides from the 5' end of DNA double-stranded substrates and efficiently resects structures with 5' overhanging flaps<sup>5,6</sup>. The function of EXO1 is closely related to genomic DNA metabolic processes such as replication stress response, double strand break repair, mismatch repair, nucleotide excision repair and telomere maintenance<sup>7</sup>. It was reported that EXO1 polymorphisms were associated with an increased susceptibility to cancers<sup>8,9</sup>, and high expression of EXO1 was related to poor prognosis of several cancers, including LUAD<sup>10</sup>, hepatocellular carcinoma<sup>11,12</sup>, prostate cancer<sup>13</sup> and breast cancer<sup>14</sup>.

Tissue-resident memory T ( $T_{RM}$ ) cells are a special kind of memory T cells that have been discovered in recent years. They can reside in non-lymphoid tissues without entering the bloodstream recirculation<sup>15</sup>.  $T_{RM}$  resides in multiple tissues including lung, gastrointestinal tract, skin, brain and kidney<sup>16–18</sup>.  $T_{RM}$  cells play an

<sup>1</sup>Department of Radiotherapy Oncology, Affiliated Hospital of Shandong University of Traditional Chinese Medicine, 250011 Jinan, P.R. China. <sup>2</sup>Department of Pathology, Shandong Provincial Hospital, Shandong University, 250021 Jinan, P.R. China. <sup>3</sup>Department of Pathology, Shandong Provincial Hospital Affiliated to Shandong First Medical University, 250021 Jinan, P.R. China. <sup>4</sup>Department of Respiratory and Critical Care Medicine, Affiliated Hospital of Shandong University of Traditional Chinese Medicine, 250014 Jinan, P.R. China. <sup>5</sup>Department of Oncology, The First Affiliated Hospital of Shandong First Medical University & Shandong Provincial Qianfoshan Hospital, Shandong Lung Cancer Institute, 250014 Jinan, P.R. China. <sup>6</sup>Zhuoqi Li, Xiaoyan Lin and Yuanhui Yang contributed equally to this work. ✉email: weizhigang321321@163.com; tytytianyuan@aliyun.com

important role in anti-tumoral immunology for a variety of cancers, such as lung cancer, breast cancer, intestinal cancer, ovarian cancer and melanoma<sup>19–23</sup>, and the infiltration of T<sub>RM</sub> cells in tumor tissues is a protective factor for the prognosis of patients<sup>24</sup>. Recent study has shown that T<sub>RM</sub> cells residing in specific organs play different roles, and the specific genes of T<sub>RM</sub> cells in barrier sites such as lung were obtained through the integrative analyses of single-cell proteins and transcriptome<sup>25</sup>. To explore whether the lung T<sub>RM</sub> specific genes play unique roles in the immune function of T<sub>RM</sub> cells in LUAD, we performed multi-omics bioinformatic analyses using data from multiple LUAD cohorts. We constructed a lung specific T<sub>RM</sub> related signature that can efficiently predict the prognosis and immunotherapeutic outcomes of LUAD patients, and found EXO1 was the core gene in this prognostic signature (the corresponding manuscript is under review).

Based on our previous study, to further explore the roles of EXO1 in the diagnosis and prognosis, tumor immune cell infiltration, immune checkpoints, immunotherapy, aberrant DNA methylation and genetic alterations of LUAD, we performed in-depth bioinformatics analyses in LUAD using the data from TCGA and GEO databases, and validated our results through the immunohistochemical staining experiment on clinical samples.

## Materials and methods

### Data collection and processing

The gene expression data was acquired from TCGA and GEO databases. TCGA Pan-Cancer (PANCAN) dataset including TCGA-LUAD was downloaded using UCSC-xena (<https://xenabrowser.net/datapages/>) website. It contains 10,535 samples including normal and tumor tissues, and the clinical information, including OS of patients. The TCGA data was normalized to  $\log_2(\text{TPM} + 1)$ . The GSE32863, GSE43458, GSE116959, GSE135222, GSE162945 and GSE203360 datasets were downloaded from GEO (<https://www.ncbi.nlm.nih.gov/geo/>) database. Among them the GSE162945 dataset consisted of nine samples receiving radiotherapy and nine samples without radiotherapy. GSE135222 is an immunotherapeutic cohort containing 27 NSCLC patients treated with anti-PD-1/PD-L1 drugs. GSE203360 contained the scRNA data of six LUAD samples. The other four datasets all contained normal lung tissues and LUAD tissues.

### Analyzing EXO1 expression in normal and cancer tissues

TCGA Pan-Cancer (PANCAN) dataset was applied to investigate EXO1 expression between normal and tumor tissues in multiple cancer types. TCGA-LUAD, GSE32863, GSE43458 and GSE116959 datasets were used to analyze EXO1 expression levels in normal lung and LUAD tissues. DESeq2-count or Mann-Whitney U test- $\log_2\text{TPM}$  was served to calculate the significance.

### Identification of differentially expressed genes (DEGs)

The patients in TCGA-LUAD dataset were divided into EXO1 low expression and high expression groups according to the median expression level. R package “limma” was used to screen differentially expressed genes between EXO1 low and high expression level, with the threshold set at  $p < 0.05$  and  $|\log\text{FC}| > 1$ . The volcano plot and heatmap were used to show the DEGs. GO and GSEA analyses were subsequently performed for these DEGs.

### Biological functional annotation

R package “clusterProfiler” was applied to perform the GO enrichment analysis. The Gene Set Variation Analysis (GSVA) algorithm was used to calculate the score for each KEGG pathway in each sample. The differentially activated pathways in EXO1 expression high and low groups were identified using the “limma” package with the differential threshold set at  $\text{FDR} < 0.05$ . Differentially activated REACTOME pathways between EXO1 expression high and low groups were analyzed using Gene Set Enrichment Analysis (GSEA).

### Single-cell RNA-seq (scRNA-seq) analysis

The R package “Seurat” was used to preprocess the scRNA-seq data. Cells with more than 50 and less than 10,000 genes and with less than 5% mitochondrial gene expression were included in this study. The “NormalizeData” function was used to normalize the scRNA-seq dataset, and 1500 highly variable genes was identified using the “vst” method of the “FindVariableFeatures” function. Subsequently, we made scale transformed for the data and performed principal component analysis (PCA) for dimensionality reduction. We eventually selected the top 20 principal components for the downstream analyses. We then used the TSNE algorithm for cell clustering analysis and the visualization of the results. The cell types were annotated through R package “SingleR”.

### The evaluation of immune microenvironment in LUAD

The marker genes of 28 immune cell types were obtained from the TISIDB (<http://cis.hku.hk/TISIDB/>) database, and the infiltration status of immune cell types in LUAD tissues was assessed using ssGSEA. The correlation between EXO1 expression and immune cell infiltration was evaluated by Spearman correlation analysis. The immune checkpoint genes were got from a publication<sup>26</sup>, and Spearman analysis was also used to calculate the correlation between the expression of EXO1 and immune checkpoint genes.

### Methylation, mutation and CNV analyses

Online tool MetSurv (<https://biit.cs.ut.ee/methsurv/>) was used to analyze the DNA methylation level of EXO1 gene and the prognostic value of EXO1 CpG islands. The CNV data of TCGA-LUAD was downloaded using TCGAbiolinks, and then the CNV frequent was presented in a plot finished by R software. The effects of copy number variation and somatic mutations in EXO1 on prognosis were also evaluated according to patients' survival time.

### The association between EXO1 and patient clinical features

The correlation between EXO1 high and low expression groups and clinical features was assessed according to patient clinical information. The logistic analysis was used to analysis the correlation between EXO1 expression levels and clinical features. KM curve was applied to analyze patients' prognosis in EXO1 high and low groups. The univariate and multivariate Cox regression analyses were employed to figure out whether EXO1 is an independent risky factor for LUAD.

### Clinical sample collection and immunohistochemistry

Lung adenocarcinoma samples were collected from the pathological department of Shandong Provincial Hospital from 2017 to 2021. Written informed consents were provided by all participants. Tumor tissues were obtained from biopsy excision, formalin fixed and paraffin embedded (FFPE) for histological evaluation. After paraffin wax removal and rehydration, the sections were placed in Citrate Antigen Retrieval Solution, boiled for 15 min for antigen retrieval. Then, endogenous peroxidase blocker was added to block the endogenous peroxidase in the sections. After Incubated in the room temperature for 30 min, each sample was added with 50 $\mu$ L goat serum working fluid and placed in 37 $^{\circ}$ C for 20 min to block non-specific staining. Subsequently, Sections were placed on the primary antibody (Rabbit Anti-Exonuclease 1 polyclonal antibody, 1:400, bs-13119R, Bioss Ltd, CHN) for 1 h at 37 $^{\circ}$ C. After 3 $\times$ 5-minute PBS solution washes, the sections were incubated in biotinylated secondary antibody at room temperature for 30 min, followed by subsequent washes (3 $\times$ 5 min in PBS solution). Then, the sections were dried with absorbent paper and incubated with 50 $\mu$ L horseradine-labeled streptin for 20 min at 37 $^{\circ}$ C. The sections were then rinsed with PBS solution for 3 $\times$ 5 min. After immunostaining, the sections were visualized using a MBMbio-intelligence-400 scanner according to the manufacturer's protocol. Slides were examined by two experienced pathologists independently according to WHO criteria.

### Statistical analysis

All the bioinformatic analyses were performed in R software (version 4.4.0). For significance analysis between various values, the wilcoxon rank-sum test was applied to compare the differences between two groups of samples, while Kruskal-Wallis test was used to compare the differences between multiple groups of samples. For plot presentation, the "ns" represents  $p > 0.05$ ; \* represents  $p < 0.05$ ; \*\* represents  $p < 0.01$ ; \*\*\* represents  $p < 0.001$ ; and \*\*\*\* represents  $p < 0.0001$ . Survival curves in the prognostic analysis were generated by the Kaplan-Meier method, and the significance of the differences was determined by the log-rank test.

## Results

### The aberrant expression of EXO1 in LUAD and the exploration of its influence factors

The pan-cancer data in TCGA were downloaded from the UCSC-xena database, in which there were 33 cancer types. The expression data were normalized to  $\log_2(\text{TPM} + 1)$  to compare the differential expression of EXO1 gene in cancer and adjacent normal tissues in each cancer type (Fig. 1A). The LUAD data was extracted from the pan-cancer data, with a total of 572 samples, 513 being cancer samples and 59 being normal tissues. Results showed the expression level of EXO1 was significantly higher expressed in LUAD compared with normal tissues (Fig. 1B). Moreover, we obtained multiple datasets containing both LUAD tissues and adjacent normal tissues from GEO database including GSE32863, GSE43458 and GSE116959. The expression level of EXO1 was also higher in LUAD according to the analytical results in these datasets (Fig. 1C-E).

To research whether the expression of EXO1 was regulated by copy number variation (CNV) in LUAD, CNV analysis was performed based on the data downloaded using TCGAAbiolinks. The proportion of every EXO1 CNV pattern was presented in Supplementary Fig. 1A. EXO1 expression was upregulated in the EXO1 gain and deletion groups compared with diploid group, but there was no significant difference between EXO1 gain and deletion groups (Supplementary Fig. 1B). This may mean EXO1 expression was not regulated by CNV.

To investigate whether radiotherapy could affect the expression of EXO1 in LUAD, the expression level of EXO1 in LUAD patients receiving radiotherapy or not receiving radiotherapy was analyzed in GSE162945 dataset. Results showed EXO1 expression was significantly downregulated after radiotherapy (Fig. 1F).

### EXO1 expression levels were associated with clinicopathological characteristics

Correlation analysis was performed to research the association between EXO1 expression levels and clinicopathological characteristics in LUAD patients. Results showed there were significant differences in clinical stages, TNM stages, overall survival (OS) and smoke rate between EXO1 high and low expression groups (Table 1). EXO1 expression levels showed a significant correlation with the clinical stages (Fig. 2A), TNM stages (Fig. 2B-D), overall survival (OS) (Fig. 2E), disease specific survival (DSS) (Fig. 2F), disease free interval (DFI) (Fig. 2G) and progression free interval (PFI) (Fig. 2H). The logistic regression analysis showed the expression level of EXO1 was correlated with multiple clinicopathological features such as clinical stages, TNM stages, gender, tumor status, smoke and age (Table 2).

### EXO1 was a potential biomarker for the diagnosis and prognosis prediction of LUAD

To investigate the value of EXO1 in the diagnosis and prognosis prediction for LUAD patients, Kaplan-Meier survival analysis and correlation analysis between EXO1 expression and patient clinical features were performed. Patient prognosis between EXO1 high and low expression groups was analyzed based on OS, DSS, PFI and DFI, respectively. Results showed patients with high EXO1 expression had significantly worse prognosis for OS (Fig. 3A), DSS (Fig. 3B) and PFI (Fig. 3D), but not for DFI (Fig. 3C). Subsequently, univariate and multivariate Cox regression analyses were conducted, and results showed EXO1 was an independent risk factor in the prediction of OS among other clinical features such as gender and TNM stage (Table 3).

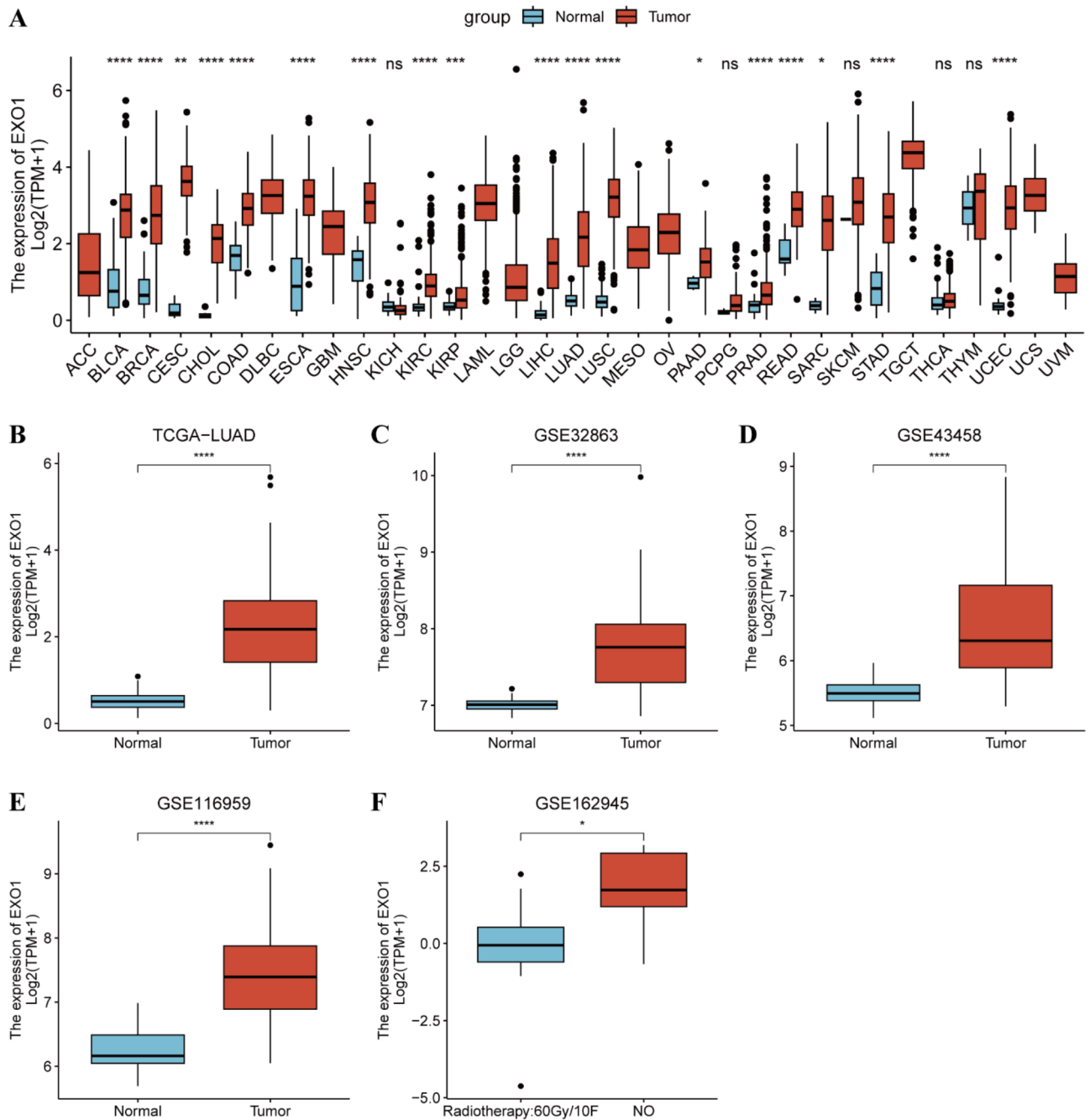


**Fig. 1.** EXO1 expression significantly up-regulated in multiple cancers including LUAD. (A) The differences of EXO1 expression between tumor and adjacent normal tissues in pan-cancer types. (B-E) EXO1 expression levels were significantly higher in the LUAD tissues compared to the adjacent normal lung tissues in the TCGA-LUAD (B), GSE32863 (C), GSE43458 (D) and GSE116959 (E) datasets. (F) EXO1 expression was downregulated in LUAD patients receiving radiotherapy. DEGs, differentially expressed genes. \* $p < 0.05$ ; \*\* $p < 0.01$ ; \*\*\* $p < 0.001$ ; \*\*\*\* $p < 0.0001$ .

ROC curve analysis was used to determine the diagnostic value of EXO1 expression levels, which could accurately differentiate between tumor and adjacent normal tissues with an AUC value of 0.962 (Fig. 4A). The time-dependent ROC curve analysis was used to evaluate the efficacy of EXO1 expression in predicting the prognosis of LUAD patients, and the results showed the AUC value at 1-, 3-, and 5-year survival was 0.628, 0.636 and 0.599, respectively (Fig. 4B). A nomogram model was constructed that included EXO1 expression levels, clinical stages, TNM stages, tumor status, age and smoke as parameters. These factors were established as highly significant prognostic prediction factors based on the multivariate Cox regression analysis. The nomogram showed a significantly high clinical value in predicting the 1-, 3-, and 5-year survival probability of the LUAD patients (Fig. 4C).

Characteristic	high_EXO1 expression	low_EXO1 expression	<i>p</i>
Total number of patients	258	255	
Age (mean (SD))	64.24 (10.05)	66.33 (9.95)	0.021
Gender (%)			0.029
Female	126 (48.8)	150 (58.8)	
Male	132 (51.2)	105 (41.2)	
Race (%)			0.905
Asian	5 (1.9)	3 (1.2)	
Black or African American	27 (10.5)	25 (9.8)	
others	33 (12.8)	33 (12.9)	
White	193 (74.8)	194 (76.1)	
Clinical stage (%)			0.001
Stage I	121 (46.9)	161 (63.1)	
Stage II	67 (26.0)	55 (21.6)	
Stage III	52 (20.2)	31 (12.2)	
Stage IV	18 (7.0)	8 (3.1)	
T stage (%)			0.037
T1	71 (27.5)	101 (39.6)	
T2	152 (58.9)	124 (48.6)	
T3	25 (9.7)	22 (8.6)	
T4	10 (3.9)	8 (3.1)	
N stage (%)			0.025
N0	157 (60.9)	184 (72.2)	
N1	52 (20.2)	44 (17.3)	
N2	48 (18.6)	26 (10.2)	
N3	1 (0.4)	1 (0.4)	
M stage (%)			0.043
M0	240 (93.0)	248 (97.3)	
M1	18 (7.0)	7 (2.7)	
OS event (%)			0.014
Alive	150 (58.1)	176 (69.0)	
Death	108 (41.9)	79 (31.0)	
DSS event (%)			0.051
Alive	171 (71.8)	191 (79.9)	
Death	67 (28.2)	48 (20.1)	
DFI event (%)			0.302
Alive	95 (67.4)	119 (73.5)	
Death	46 (32.6)	43 (26.5)	
PFI event (%)			0.132
Alive	144 (55.8)	160 (62.7)	
Death	114 (44.2)	95 (37.3)	
Tumor status (%)			0.063
Tumor free	132 (51.2)	155 (60.8)	
Unknow	29 (11.2)	28 (11.0)	
With tumor	97 (37.6)	72 (28.2)	
KRAS mutation performed (%)			0.07
NO	234 (90.7)	217 (85.1)	
YES	24 (9.3)	38 (14.9)	
EGFR mutation performed (%)			0.858
NO	219 (84.9)	214 (83.9)	
YES	39 (15.1)	41 (16.1)	
Smoked (%)			0.035
NO	174 (67.4)	148 (58.0)	
YES	84 (32.6)	107 (42.0)	
Site (%)			0.069
Lower	79 (30.6)	95 (37.3)	
Middle	19 (7.4)	18 (7.1)	
Continued			

Characteristic	high_EXO1 expression	low_EXO1 expression	p
Overlapping	0 (0.0)	4 (1.6)	
Upper	160 (62.0)	138 (54.1)	

**Table 1.** Clinicopathological characteristics of LUAD patients with high- and low-EXO1 expression levels.

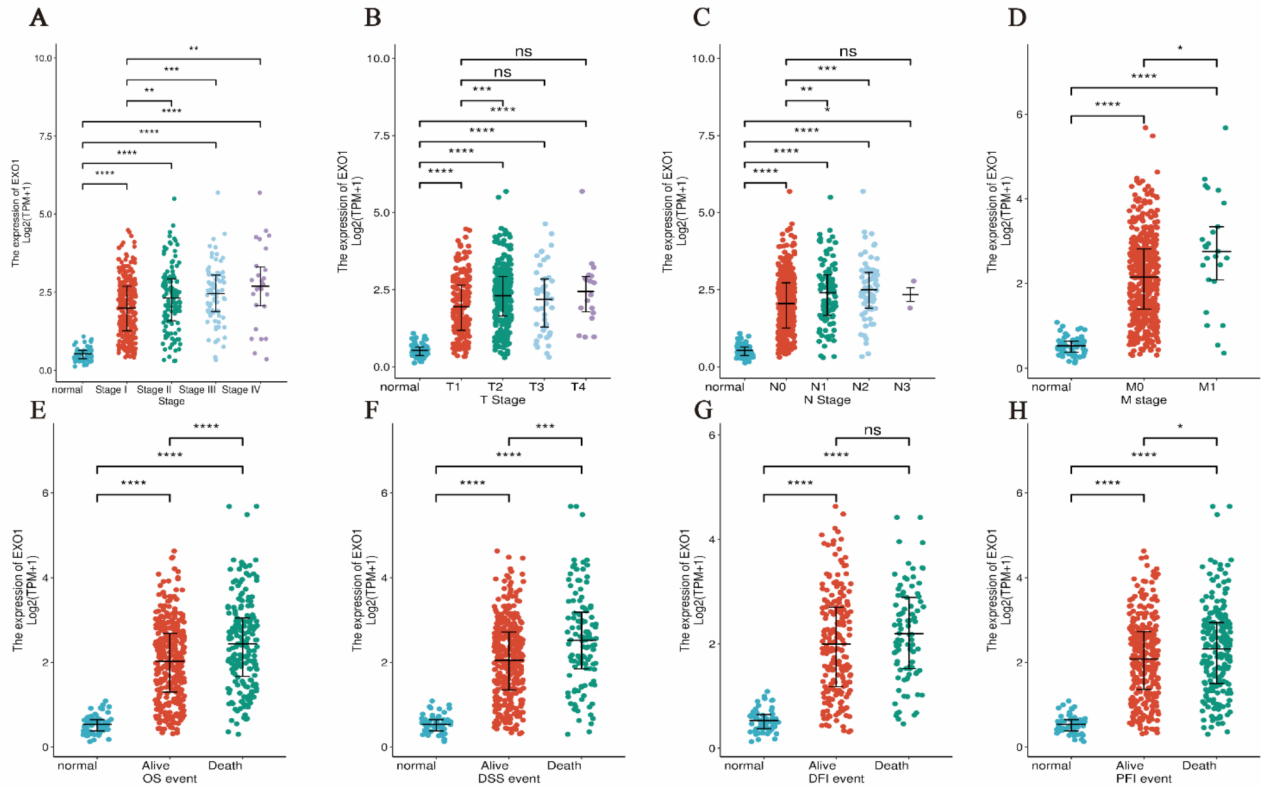


**Fig. 2.** EXO1 expression levels were correlate with multiple clinicopathological characteristics of LUAD patients. (A–H) The correlation analysis between EXO1 expression levels and clinical stages (A), T stages (B), N stages (C), M stages (D), OS status (E), DSS status (F), DFI status (G) and PFI status (H). OS, overall survival; DSS, disease specific survival; DFI, disease free interval; PFI, progression free interval. \* $p < 0.05$ ; \*\* $p < 0.01$ ; \*\*\* $p < 0.001$ ; \*\*\*\* $p < 0.0001$ .

Characteristics	OR	CI lower	CI upper	P value
Clinical stage (Stage I&II vs. Stage III&IV)	1.496598637	1.056583259	2.12431462	0.023544351
Gender (Male vs. Female)	0.484920635	0.310860543	0.747493215	0.001191802
T stage (T1 vs. T2, T3&T4)	0.578916715	0.398523444	0.837534346	0.003879704
N stage (N0 vs. N1 N2&N3)	0.599817047	0.413007516	0.86764381	0.006896574
M stage (M0 vs. M1)	0.376344086	0.144091466	0.880805431	0.031558828
Tumor status (With tumor vs. Tumor free)	0.632125046	0.430007804	0.926049477	0.018975958
Smoked (YES vs. NO)	1.49758687	1.04575797	2.150109626	0.027936244
Age (>73 vs. <=73)	1.748062016	1.137328677	2.709427676	0.011498054

**Table 2.** Logistic regression analysis of the relationship between clinicopathological and the EXO1 expression levels in LUAD patients.

**Prognostic performance of EXO1 in the clinicopathological subgroups of LUAD patients**

To further evaluate the prognostic value of EXO1, Cox regression analysis was conducted for specific LUAD subgroups according to the clinicopathologic parameters. The results showed low expression of EXO1 was a protective factor in the OS (Fig. 5A), DSS (Fig. 5B) and PFI (Fig. 5D) of all the patients, patients with T2&T3&T4

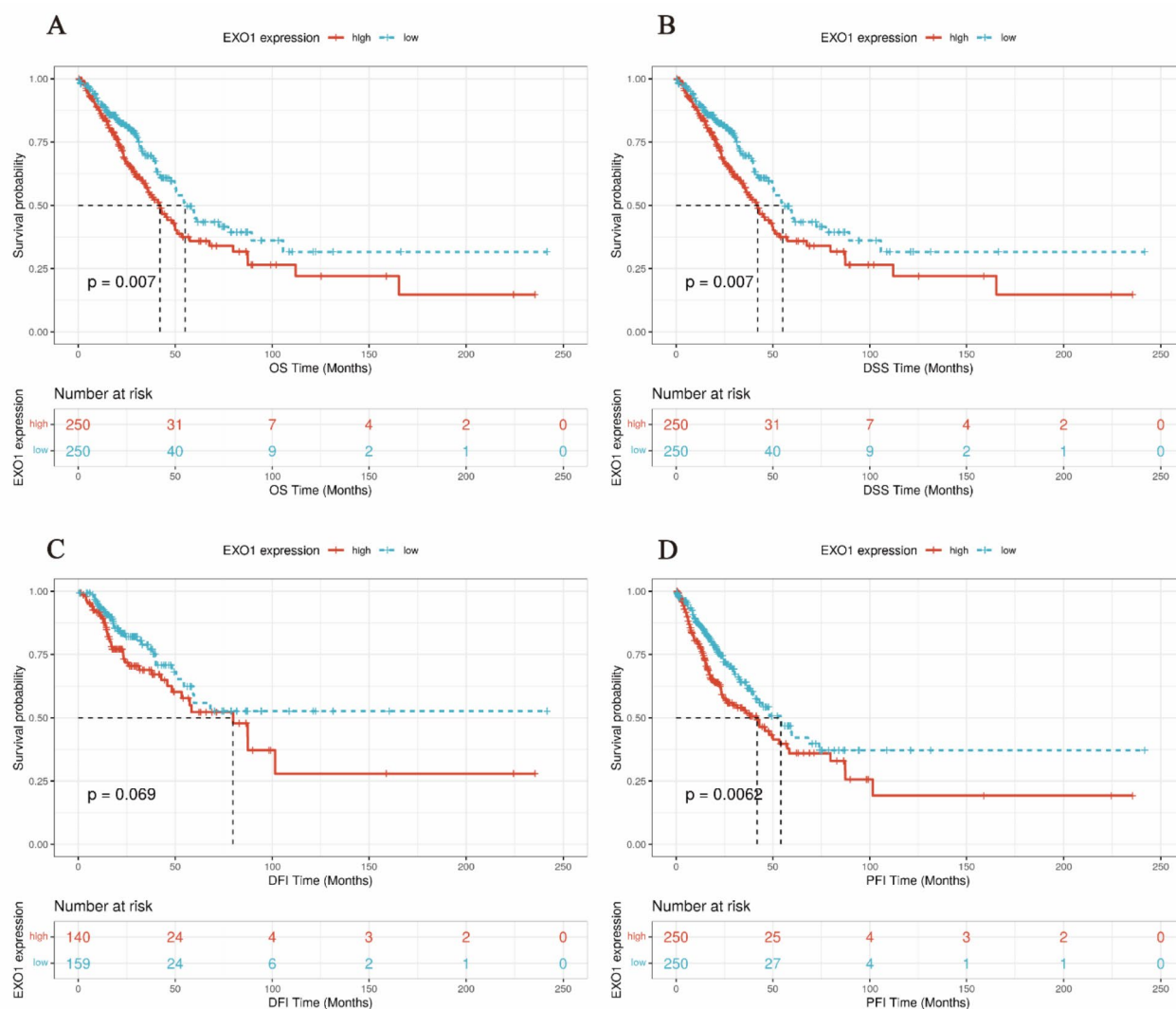


**Fig. 3.** The expression of EXO1 was associated with the prognosis of LUAD patients. (A-D) were the Kaplan-Meier curves of the patients’ overall survival (A), disease specific survival (B), disease free interval (C) and progression free interval (D).

Characteristics	HR for OS (95% CI)	
	Univariate	Multivariate
EXO1(low vs. high)	1.495(1.114–2.005)**	1.476(1.049–2.078)*
Gender (Male vs. Female)	0.947(0.707–1.268)	
Clinical stage (Stage I&II vs. Stage III&IV)	2.612(1.915–3.562)***	1.443(0.906–2.298)
T stage (T1 vs. T2, T3&T4)	1.619(1.156–2.268)**	1.12(0.76–1.65)
N stage (N0 vs. N1, N2&N3)	2.478(1.849–3.32)***	1.513(1.014–2.259)*
M stage (M0 vs. M1)	2.194(1.291–3.729)**	0.717(0.349–1.473)
Tumor status (With tumor vs. Tumor free)	6.414(4.38–9.393)***	6.121(4.134–9.062)***
Smoked (YES vs. NO)	1.13(0.831–1.535)	
Age (>73 vs. <=73)	1.339(0.957–1.874)	

**Table 3.** Cox regression analysis of the clinical in LUAD patients based on various clinicopathological characteristics including EXO1 levels.

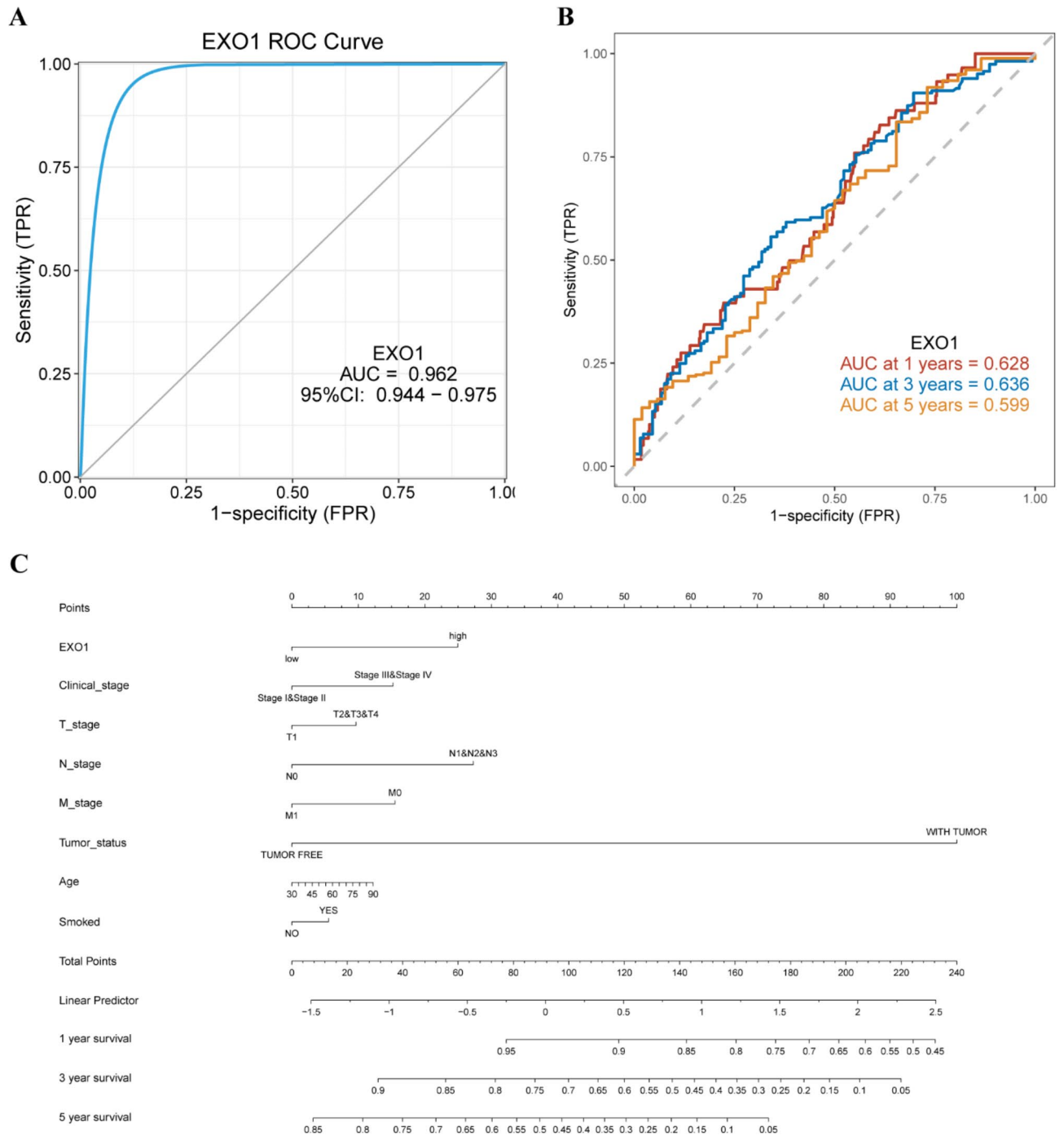


**Fig. 4.** The nomogram model with EXO1 shows a superior diagnostic and prognostic performance in LUAD. (A) Diagnostic ROC curves to distinguish LUAD tissues and normal tissues based on the EXO1 expression levels. (B) Time-dependent survival ROC curves to predict 1-, 3-, and 5-year survival rates of LUAD patients based on the EXO1 expression levels. (C) ROC curve analysis to evaluate the prediction efficacy of the nomogram model that includes EXO1 expression levels and clinicopathological factors (clinical stages, TNM stages, tumor status, age, and smoke) to predict the 1-, 3-, and 5-year survival rates of LUAD patients.

and patients with M0 stages of tumor, but not the DFI (Fig. 5C). EXO1 low expression was also favorable for the DSS (Fig. 5B), DFI (Fig. 5C) and PFI (Fig. 5D) of patients with N0 stage of tumor. Moreover, EXO1 was a protective factor for the OS (Fig. 5A), DSS (Fig. 5B), DFI (Fig. 5C) and PFI (Fig. 5D) of patients who smoked. These results demonstrated EXO1 was still a risky factor in different subgroups of LUAD patients.

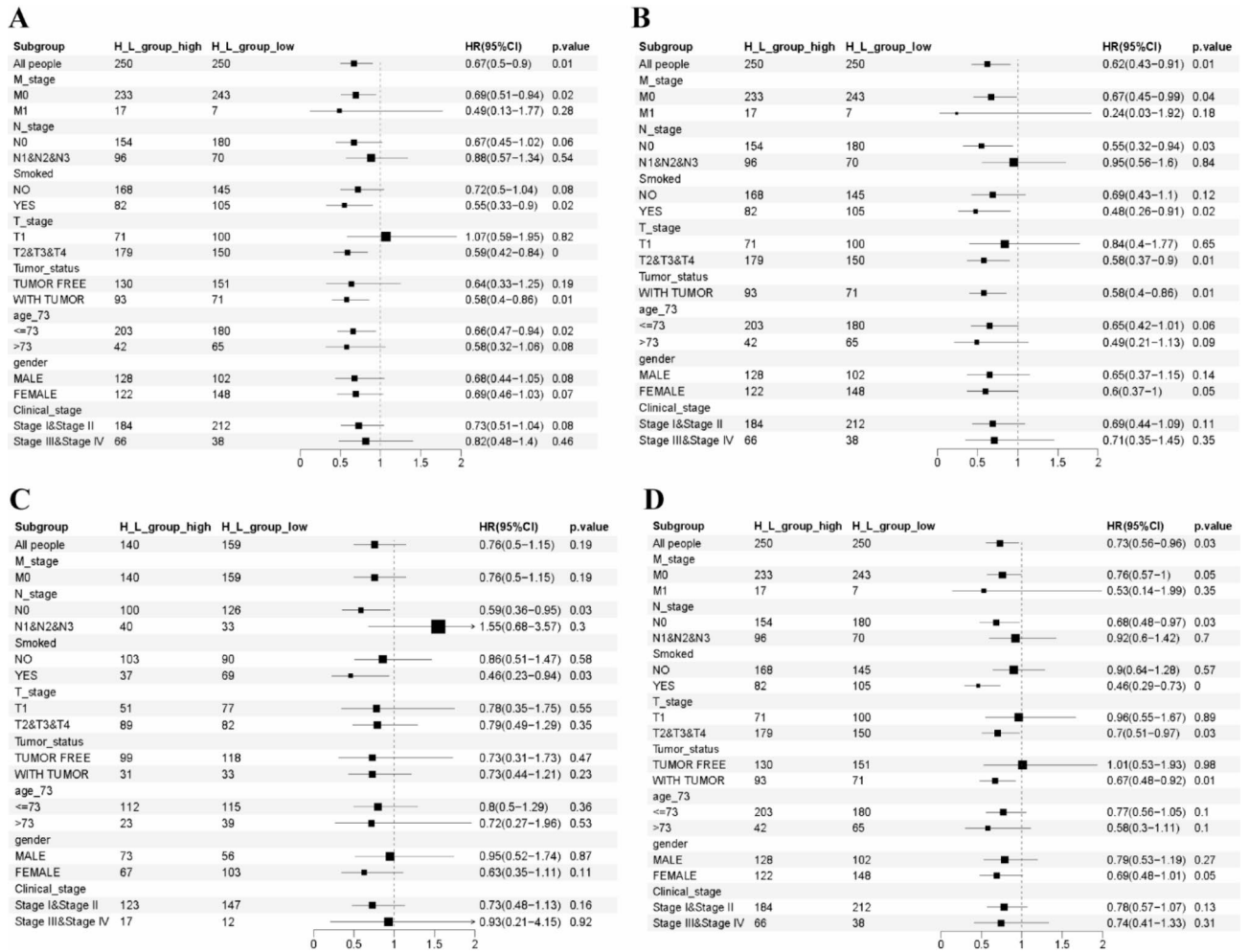


**Fig. 5.** Prognostic performance of EXO1 expression in different LUAD patient subgroups. The LUAD patients were divided into different subgroups based on TMN stages, smoke, tumor status, age, gender and clinical stages. (A–D) The Cox regression analysis results show the prognostic performance of EXO1 expression levels regarding overall survival (A), disease-specific survival (B), disease free interval (C) and progression free interval (D) in different subgroups of LUAD patients. The results are represented by the hazard ratio (HR). The ends represented the 95% confidence interval (CI) of the HR values, and the positions of the diamonds represented the significance of the prognostic performance of EXO1.

### EXO1 gene mutation, but not methylation was associated with the survival of LUAD patients

To investigate whether the genetic and epigenetic alterations of EXO1 had an impact on LUAD patients' clinical outcomes, the mutation and methylation data downloaded from TCGA was analyzed. The Kaplan-Meier curve showed patients with EXO1 mutation had significantly shorter DSS (Fig. 6B), PFI (Fig. 6C) and DFI (Fig. 6D), but the result of OS was not significant (Fig. 6A).

In the analysis of EXO1 DNA methylation by MetSurv tool, it can be observed that in UCSC\_CpG\_Island the CpG level in the Open\_Sea region was significantly higher than that in other regions (Supplementary Fig. 2). In the prognostic analysis for the CpG islands in EXO1 gene, results showed the CpG islands in EXO1 gene had no significant effect on the prognosis of LUAD patients (Supplementary Table 1).

### Identification of differentially expressed genes (DEGs) according to EXO1 expression

To explore the mechanisms underlying the effects EXO1 have on patient clinical outcomes, we identified DEGs between EXO1 low and high expression groups to make further analyses. The LUAD patients from TCGA were divided into EXO1 high and low expression groups according to the median. R package "limma" was applied to perform differential analysis between EXO1 high and low expression groups, with the threshold set at p-value < 0.05 and |logFC| ≥ 1. Totally, 317 DEGs were obtained, including 205 upregulated genes and 112 downregulated genes in EXO1 high expression group (Supplementary Table 1). The DEGs were visualized through volcano plot (Supplementary Fig. 3A). The heatmap showed the top 10 DEGs that were significantly correlated with the expression of EXO1 (Supplementary Fig. 3B).

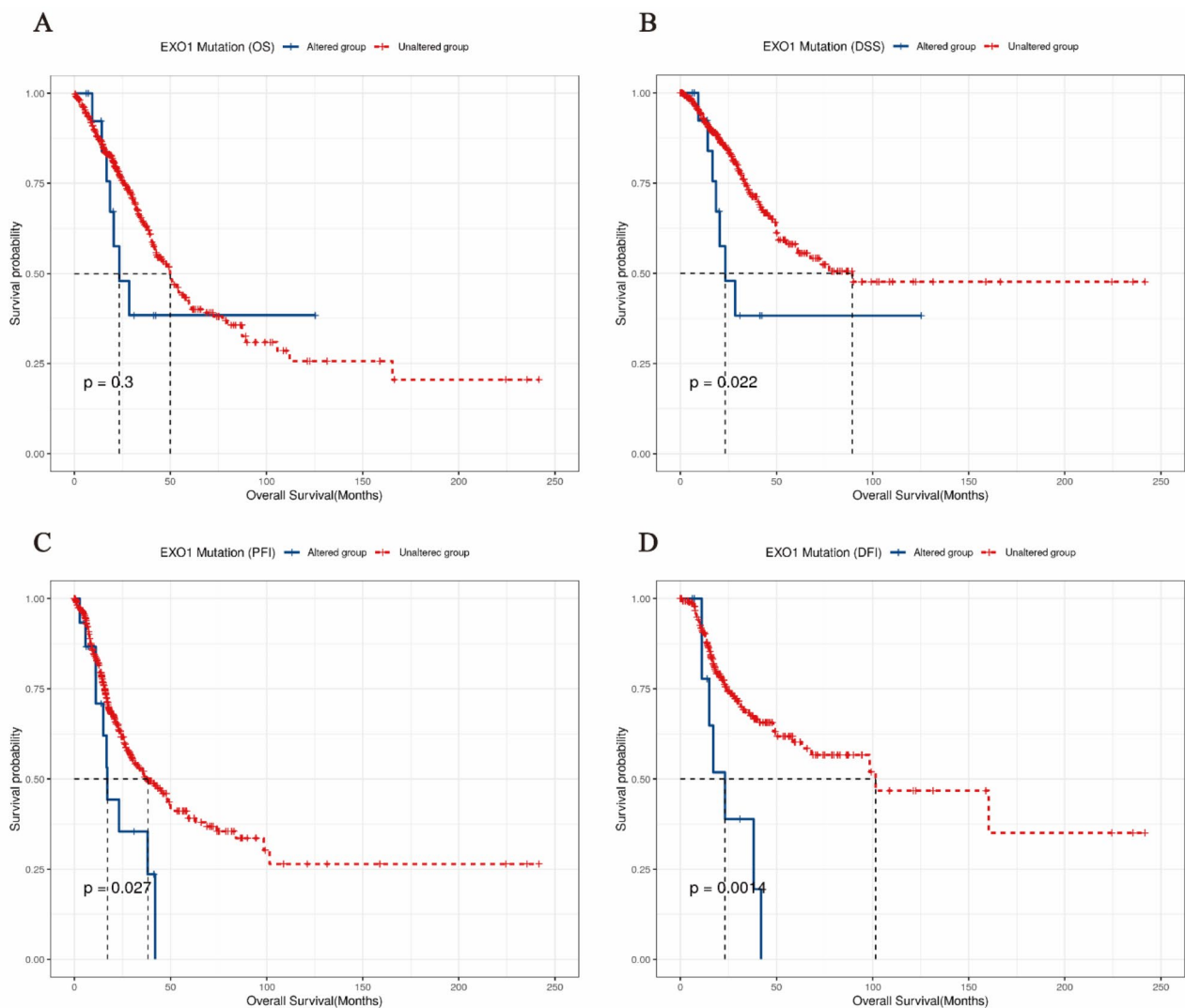


**Fig. 6.** EXO1 gene mutation was associated with the prognostic outcomes of LUAD patients. (A–D) were the Kaplan–Meier survival curves of patients’ overall survival (A), disease specific survival (B), disease free interval (C) and progression free interval (D).

### EXO1 expression levels were associated with different biological functions

R package “clusterProfiler” was applied to perform GO enrichment analysis for the 317 DEGs acquired in the last step. It could be observed the DEGs were mainly enriched in biological processes such as chromosome segregation, organelle fission and nuclear division (Fig. 7A, Supplementary Table 2). In the GSEA analysis, results showed many cancer-related pathways, such as thyroid cancer, bladder cancer and small cell lung cancer pathways were more activated in EXO1 high expression group (Fig. 7B, Supplementary Table 3). The GSEA analysis presented the DEGs were primarily enriched in pathways including Cell Cycle (Fig. 7C), Cell Cycle Mitotic (Fig. 7D), Cell Cycle Checkpoints (Fig. 7E), M Phase (Fig. 7F), Mitotic Prometaphase (Fig. 7G), Mitotic Metaphase and Anaphase (Fig. 7H), Signaling by Rho Gtpases Miro Gtpases and Rhobtb3 (Fig. 7I), Resolution of Sister Chromatid Cohesion (Fig. 7J), G2 M Checkpoints (Fig. 7K), Mitotic Spindle Checkpoint (Fig. 7L), Separation of Sister Chromatids (Fig. 7M) and Rho Gtpase Effectors (Fig. 7N). All the enriched pathways of the DEGs can be seen in Supplementary Table 4.

### The expression level of EXO1 was correlated with immune cells infiltration in LUAD

To explore the infiltration of immune cell types in different EXO1 expression groups of LUAD, ssGSEA and Spearman’s correlation analysis were performed. In the 28 types of immune cells, 20 types were significantly correlated with EXO1 expression (Fig. 8A, Supplementary Tables 5 and 6). Some tissue-resident memory T cells, such as Effector memory CD4 T cell (Fig. 8B), Effector memory CD8 T cell (Fig. 8C) and Central memory CD4 T cell (Fig. 8D) significantly differentially infiltrated in EXO1 high and low groups. Moreover, the infiltration of Activated B cell (Fig. 8E), Activated CD4 T cell (Fig. 8F) and Activated dendritic cell (Fig. 8G) were also different in two groups.

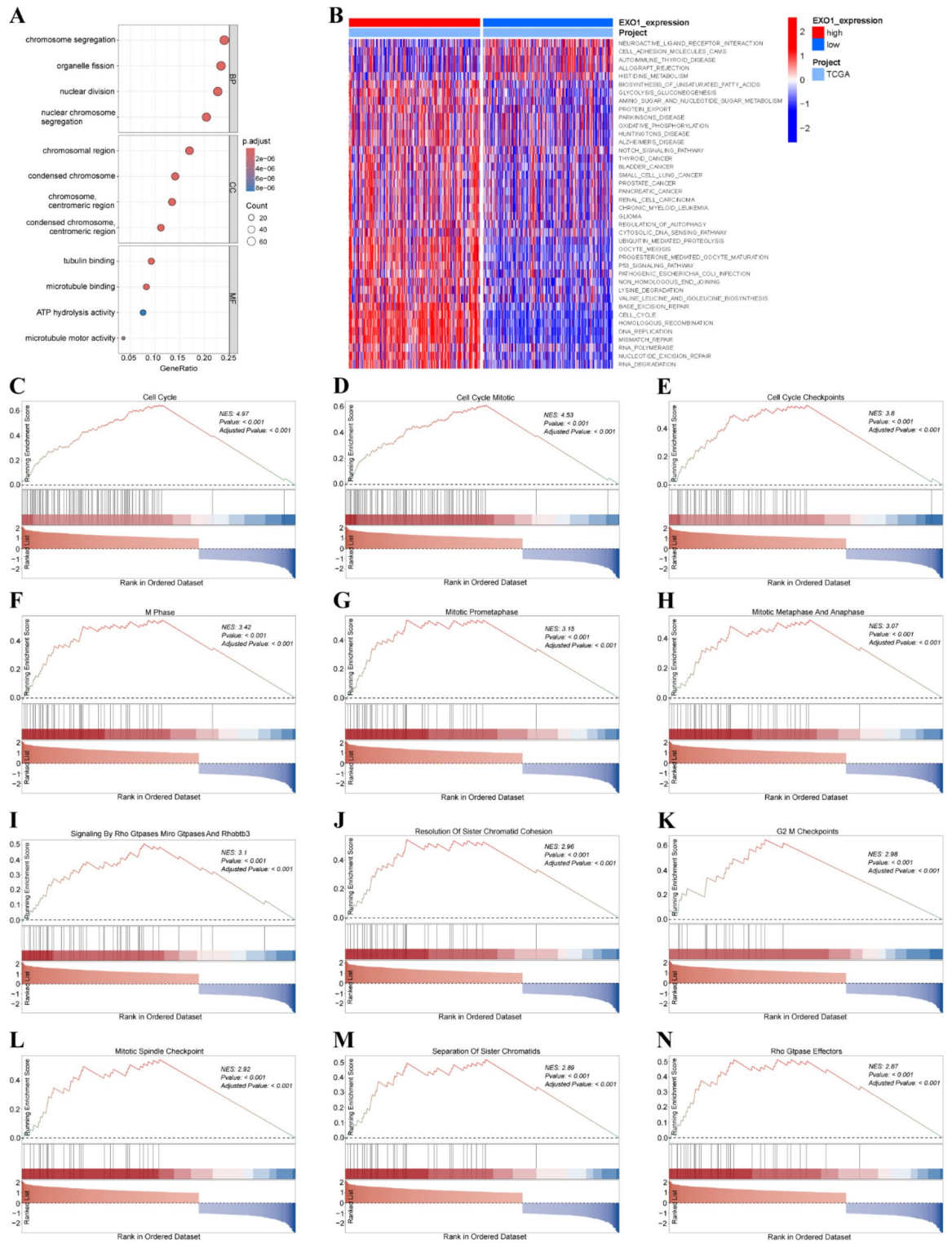


**Fig. 7.** Functional enrichment analysis of the differentially expressed genes (DEGs) between EXO1 high and low expression groups. (A) GO enrichment analysis of the EXO1-associated DEGs showed the enriched biological functions (BP), cellular components (CC) and molecular functions (MF). (B) Gene Set Variation Analysis (GSVA) of the DEGs showed the differentially activated signaling pathways between EXO1 high and low expression groups. (C–N) Gene Set Enrichment Analysis (GSEA) of the altered signaling pathways in the LUAD tissues based on the DEGs between EXO1 high and low expression groups.



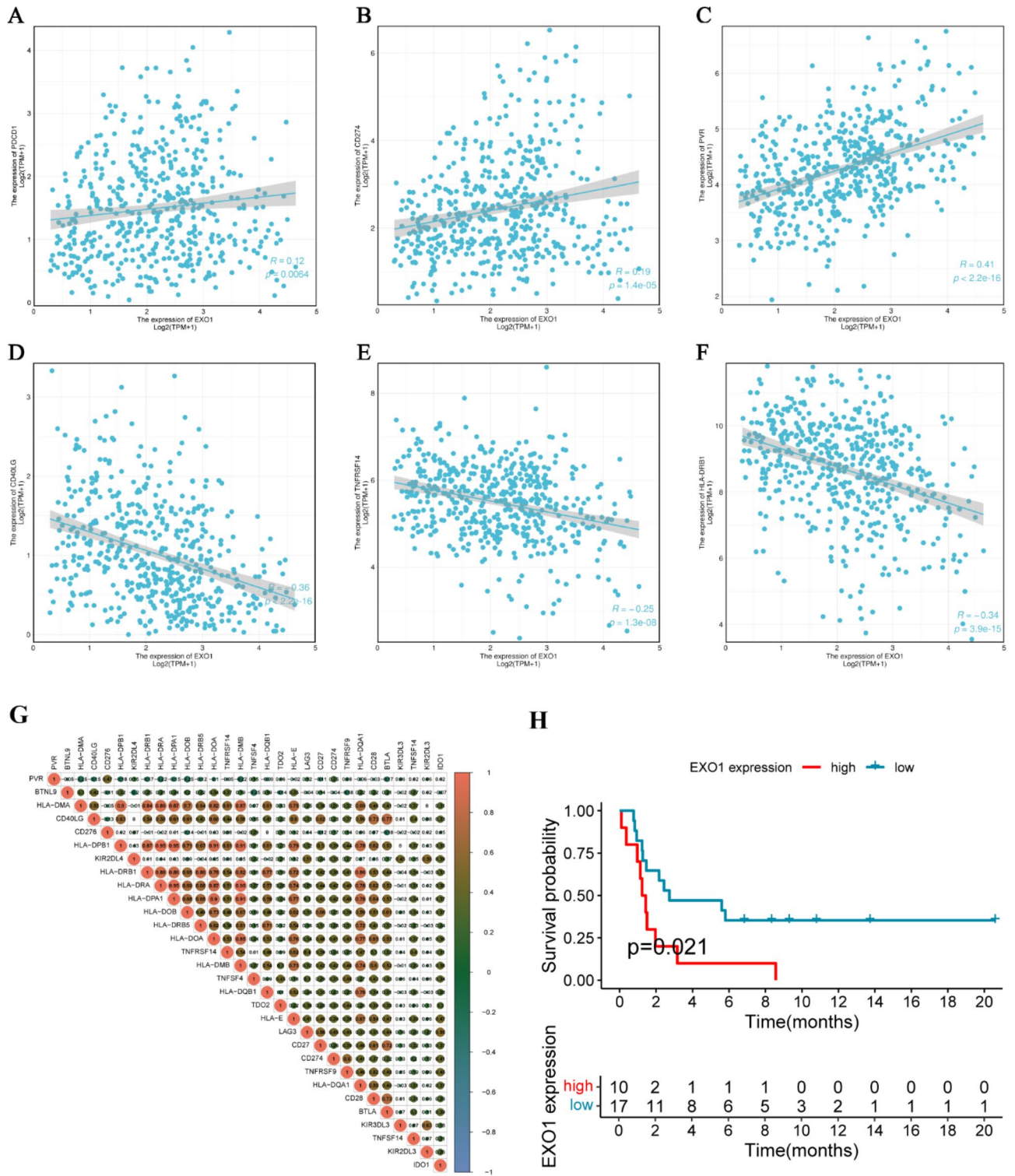


**Fig. 9.** EXO1 expression was associated with the expression of immune checkpoints and immunotherapeutic outcomes in LUAD. (A–F) The correlation analysis results between the expression levels of EXO1 and the expression levels of PDCD1LG2 (A), CD274 (B), PVR (C), CD40LG (D), TNFRSF14 (E), HLA-DRB1 (F). (G) The correlation analysis results of the top 30 mutually significantly correlated immune checkpoint genes. (H) The Kaplan–Meier survival curves showing the progression free survival of EXO1 low- and high- expression patients receiving anti-PD1/PD-L1 therapy.

to the expression of immune checkpoint genes and had an impact on the prognosis of patients treated with ICB immunotherapy.

### Analysis of EXO1 expression in single-cell data

To investigate the heterogeneity of EXO1 expression in LUAD tissues, we analyzed the single-cell RNA-seq data from GSE203360 dataset, which contained the scRNA data of six LUAD samples. The results indicated the LUAD samples can be classified into eight clusters (Supplementary Fig. 4A), and be annotated for four cell types, namely B cell, epithelial cell, macrophage and monocyte (Supplementary Fig. 4B). EXO1 mainly expressed in macrophage, the cluster 6 of cells (Supplementary Fig. 4C). The trajectory analysis indicated with time going by, the other cell clusters gradually differentiated into cluster 2 and cluster 3 (Supplementary Fig. 4D and 4 F). Correspondingly, macrophage and monocyte transformed to B cell, epithelial cell (Supplementary Fig. 4E and 4 F).

### Validation of the clinical significance of EXO1 in experimental LUAD samples

To validate the clinical significance of EXO1 we discovered previously in proteinic level, we conducted IHC staining on clinical LUAD samples and analyzed the data acquired in the experiment. The basic clinical information of the 20 LUAD patients was shown in (Table 4). Figure 10A-C were the IHC staining images of EXO1, showing no expression, low expression and high expression of EXO1 protein, respectively (Fig. 10A-C). EXO1 protein level did not significantly varied with clinical stages (Fig. 10D) and M stages (Fig. 10E), but it was prominently upregulated as N stages (Fig. 10F) and T stages (Fig. 10G) advanced. The Kaplan-Meier survival analysis confirmed our former results that high expression of EXO1 was a risky factor for the prognosis of LUAD patients (Fig. 10H).

### Discussion

In our study, we found EXO1 was aberrantly upregulated in multiple kinds of tumors including LUAD (Fig. 1A-E). High expression of EXO1 was associated with shorter survival time of LUAD patients (Fig. 3A-D), and Cox regression analysis also showed high expression of EXO1 was a risky factor for patients' prognosis (Table 3). Moreover, EXO1 expression was correlated with various clinicopathological characteristics such as clinical stages and TNM stages (Tables 1 and 2; Fig. 2), and the expression levels of EXO1 were upregulated as clinical stages and TNM stages advanced (Fig. 2A-D). Apart from the prognostic predictive values, EXO1 expression was also an effective tool for the diagnosis of LUAD (Fig. 4A). Thus, it is necessary to further explore the regulatory mechanisms of EXO1 expression in tumors, and the mechanisms through which EXO1 affects the prognosis of patients. These may help a lot in the diagnosis and treatment of cancers including LUAD.

We investigated the association between CNV and EXO1 expression, and found patients with EXO1 deletion did not show a lower level of EXO1 expression compared with patients with EXO1 gain or diploid (Supplementary Fig. 1B). This meant the expression of EXO1 was not regulated by CNV. There were a few studies about EXO1 expression regulation. EXO1 can be upregulated by some transcription factors like FOXP3 and FBXO32, which could promote the progression of HCC, and facilitate the insensitivity of osteosarcoma to radiotherapy, respectively<sup>12,27</sup>. EXO1 levels can also be regulated by some post-translational protein modification such as phosphorylation and sumoylation<sup>28,29</sup>. However, the mechanisms about the upregulation of EXO1 in many

Characteristics	Levels	Overall
n		20
Age, n (%)	<60	6 (30)
	≥60	14 (70)
Gender, n (%)	Male	14 (70)
	Female	6 (30)
Smoker, n (%)	No	9 (45)
	Yes	11 (55)
T stage, n (%)	T1	3 (15)
	T2	4 (20)
	T3	7 (35)
	T4	6 (30)
N stage, n (%)	N0	1 (5)
	N1	2 (10)
	N2	8 (40)
M stage, n (%)	N3	9 (45)
	M0	6 (30)
	M1	14 (70)
Clinical stage	I	1 (5)
	II	1 (5)
	III	4 (20)
	IV	14 (70)

**Table 4.** The basic clinical information of the patients enrolled in the experiments.

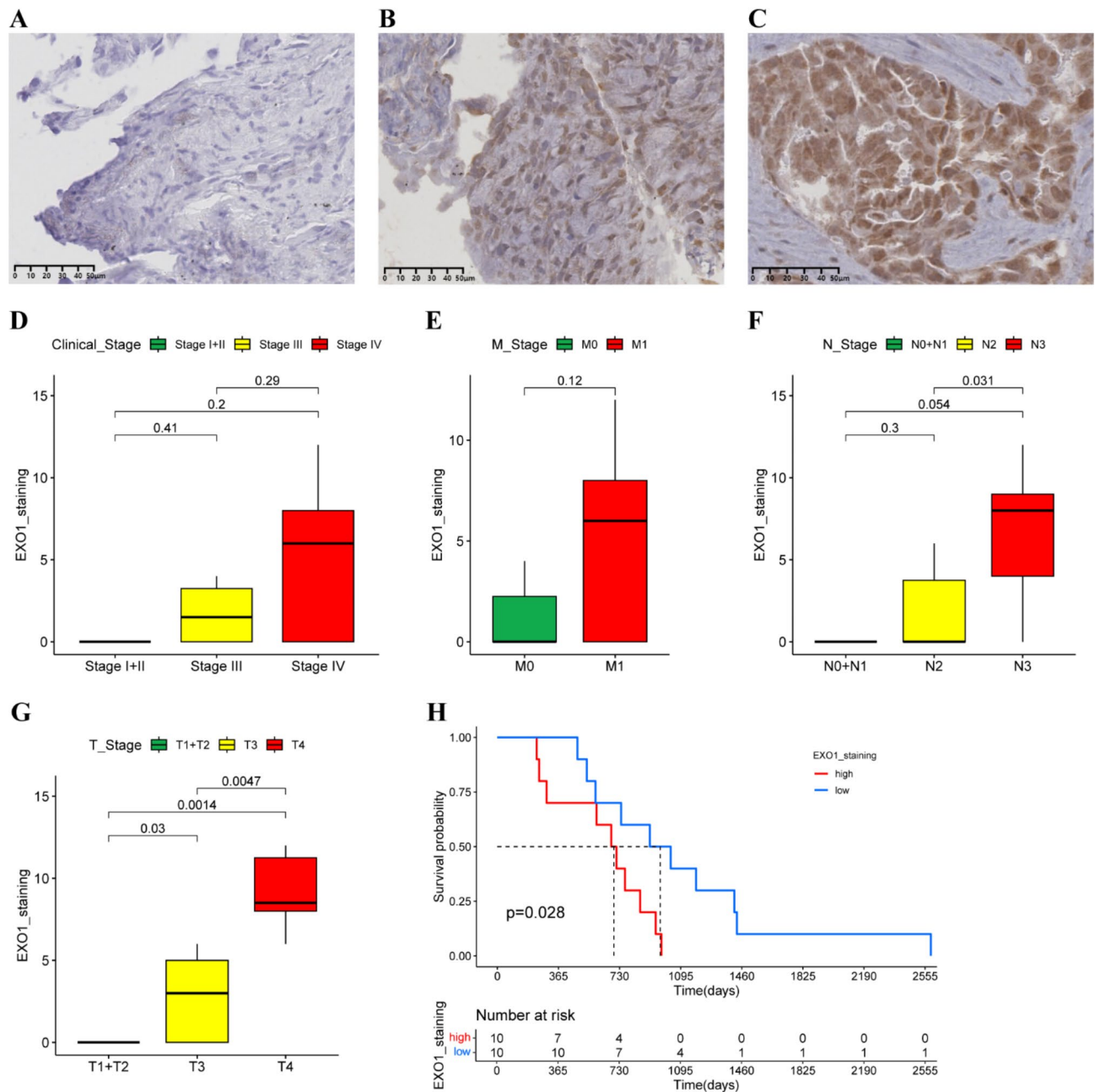


**Fig. 10.** Validation of the clinical significance of EXO1 in LUAD clinical samples. (A–C) Representative photomicrographs of EXO1 protein expression by immunohistochemical (IHC) staining, showing no expression (A), low expression (B) and high expression (C) of EXO1 protein. (D–G) Box plots showing the association between EXO1 expression and the clinical stages (D), M stages (E), N stages (F) and T stages (G). (H) The Kaplan–Meier survival curves showing the overall survival of LUAD patients with low and high EXO1 protein expression in clinical samples.

cancers including LUAD still need to be better clarified. Previous studies demonstrated EXO1 was associated with resistance to radiotherapy<sup>30,31</sup>. In our study, we found radiotherapy could reduce the expression of EXO1 (Fig. 1E), but there was no report that could elucidate the mechanisms about the effect radiotherapy had on EXO1 expression. This need to be further studied. Patients with EXO1 mutation showed poorer prognosis in our analysis (Fig. 6A–D). There was no study about the roles of EXO1 mutation in LUAD, but certain types of EXO1 single nucleotide polymorphism (SNP) were reported to be associated with high risk of cancers development<sup>8,9,32</sup>. The underlying mechanisms also require further exploration.

The mechanisms about how EXO1 affect the clinical outcomes of LUAD patients have been rarely reported. EXO1 expression levels were elevated during cell cycle progression and cell proliferation, thus high expression of EXO1 may be related to the vigorous proliferation of tumor cells<sup>33</sup>. It has also been suggested that EXO1 promotes the expression of SREBP1 by inhibiting P53 signaling pathway, thereby regulating lipid metabolic

reprogramming of prostate cancer cells and promoting the progression of prostate cancer<sup>13</sup>. To further explore the mechanisms, we performed functional enrichment analysis based on the EXO1-related DEGs and evaluated the immune cell infiltration in the LUAD samples (Figs. 7 and 8). KEGG (Kyoto Encyclopedia of Genes and Genomes) is a knowledge base for systematic analysis of gene functions, linking genomic information with higher order functional information<sup>34</sup>. The GSEA was performed using the PATHWAY database of KEGG. The results showed multiple cancer-related pathways were more active in LUAD samples with high EXO1 expression, including small cell lung cancer (SCLC), bladder cancer, prostate cancer, pancreatic cancer and so on (Fig. 7B). This was consistent with the previously published studies<sup>13,14,35</sup>. Although the non-small cell lung cancer pathway did not show up in the GSEA results (Fig. 7B), some key genes or signaling pathways involved in other types of cancer were also closely related to the development of LUAD. For example, MYC was an important oncogene for the development of small cell lung cancer<sup>36</sup>. The copy number amplification and aberrant high expression of MYC was closely associated with the progression and metastasis of LUAD<sup>37</sup>. Additionally, it was also an important way for MYC to promote the progression of cancer by regulating the tumor microenvironment (TME). Studies have pointed out that MYC facilitated the angiogenesis, the infiltration of immune suppressive stromal cells and the exclusion of adaptive T and B cells through coaction with KRAS, which made the inert LUAD become highly proliferative and invasive<sup>38</sup>. Actually, LUAD can also transform to SCLC. It usually occurs in epidermal growth factor receptor (EGFR) mutant LUAD after treatment with tyrosine kinase inhibitors (TKIs)<sup>39,40</sup>. Therefore, the activation of SCLC pathway by high expression of EXO1 could also contribute to the progression of LUAD.

In the REACTOME pathway GSEA for the EXO1-related DEGs, the results showed the DEGs were enriched in cell cycle checkpoints (Fig. 7E). Thus, we investigate the correlation between the expression levels of EXO1 and immune checkpoint genes (Fig. 9A-F, Supplementary Table 8). Although EXO1 expression was positively correlated with the expression of PDCD1 (PD-1) and CD274 (PD-L1) in LUAD (Fig. 9A-B), patients with high EXO1 expression had inferior prognosis compared with patients with low EXO1 expression in an anti-PD-1/PD-L1 immunotherapeutic cohort (Fig. 9H). It was also reported that EXO1 can activate the cGAS-STING pathway, which could strengthen the efficacy of tumor immunotherapy, through increasing single-strand DNA formation, RPA exhaustion, DNA breaks, and aberrant DNA repair intermediates<sup>41</sup>. These suggested that EXO1 was a potential target for improving the efficacy of ICB immunotherapy for LUAD patients.

The TME played crucial roles in regulating tumor development and modulating response to therapies, and immune cells were important composition of the TME<sup>42,43</sup>. According to the results, EXO1 expression levels were negatively correlated with most of the immune cell types involved in our study (Fig. 8A), including Effector memory CD8 T cell (Fig. 8C) and Central memory CD4 T cell (Fig. 8D), the two major kinds of T<sub>RM</sub>. Actually, in our previous study, we constructed a lung specific T<sub>RM</sub>-related gene signature that could effectively depict the TME landscape and predict the prognosis of LUAD patients, and EXO1 was the core gene of the prognostic signature (the corresponding manuscript has not been published by a journal). T<sub>RM</sub> cells played vital roles in antitumor immune response<sup>19–23</sup>. The abundance of CD103+CD8+T<sub>RM</sub> cells in tumor tissues was positively correlated with the survival time of patients with multiple types of cancer including LUAD<sup>44–48</sup>. The reasons may be that CD8+T<sub>RM</sub> cells could directly inhibit the growth of tumor cells and kill them by secreting cytokines like IFN- $\gamma$ , TNF- $\alpha$ , perforin-1 and granzyme B<sup>24,44,49</sup>. In the meantime, they released chemokines including CCL3, CCL4 and XCL1 that recruited DCs to tumor tissues to enhance anti-tumor immune responses<sup>24,50</sup>. Based on the above results, we speculated that EXO1 could promote the exclusion of T<sub>RM</sub> cells and reduce the infiltration of T<sub>RM</sub> cells in LUAD tissues, which impaired the anti-tumor immunology and the prognosis of patients.

Given that tumor samples were usually accompanied with temporal and spatial heterogeneity<sup>51,52</sup>, single-cell data analysis was conducted to detect the expression of EXO1 in different kinds of cells in LUAD samples. The results showed EXO1 was mainly expressed in macrophages (Supplementary Fig. 4B-C). Tumor-associated macrophages (TAM) were usually regarded as the contributors of tumor growth, metastasis, and immunosuppression<sup>53–55</sup>. Thus, EXO1 expressed in TAMs may play some roles in the tumor promotion functions of TAMs, and the specific mechanisms need to be further studied. However, a study pointed out that there is a subgroup of TAMs, namely M1<sup>hot</sup>TAMs could boost T<sub>RM</sub> cells infiltration and survival in human lung cancer<sup>56</sup>. In our analysis of the single-cell data, we found EXO1 nearly only expressed in one cluster of macrophages, called cluster 6 (Supplementary Fig. 4A-C). We consider the cluster 6 macrophage may not be M1<sup>hot</sup>TAMs.

We performed immunohistochemical staining experiments to verify the bioinformatical results. The results showed EXO1 expression levels went up in patients with higher T and N stages (Fig. 10F-G). Patients with high EXO1 expression had shorter OS time and poorer prognosis (Fig. 10H). These results from the immunohistochemical experiments were consistent with our previous results (Figs. 2 and 3), which indicated that the results of our study were reliable.

Certainly, there were some limitations in our study. First, our study was mainly based on bioinformatical analyses of public datasets, and was only partially verified by experiments on clinical tissues. Biological and molecular experiments in vitro and/or in vivo were needed to directly assess the activities of downstream signaling pathways. Second, due to our retrospective study, bias might be inevitable, and prospective experiments were needed for further validation.

## Conclusion

EXO1 was aberrantly overexpressed in multiple types of cancer including LUAD. EXO1 expression levels were correlated with many clinicopathological characteristics of LUAD and can accurately distinguish between tumor and adjacent normal tissues. High expression of EXO1 was associated with inferior prognosis for LUAD patients, the reasons may be that it was related to the activation of cancer-related pathways and the exclusion of T<sub>RM</sub> cells in tumor tissues. Moreover, the expression levels of EXO1 were correlated with these of many immune checkpoint genes, and the clinical outcomes of LUAD patients receiving ICB immunotherapy. Therefore, EXO1 was an efficient diagnostic and prognostic biomarker and a potential therapeutic target for LUAD.

## Data availability

Data that support the findings of this study were downloaded from the GEO database (<https://www.ncbi.nlm.nih.gov/gds/>) under the accession number(s) GSE32863, GSE43458, GSE116959, GSE162945 and GSE203360. The RNA-seq data, DNA methylation data, single nucleotide variation data and copy number variation data used in this study were downloaded from TCGA database (<https://portal.gdc.cancer.gov/>).

Received: 5 October 2024; Accepted: 24 January 2025

Published online: 01 February 2025

## References

- Siegel, R. L., Miller, K. D., Wagle, N. S., Jemal, A. & Cancer statistics CA Cancer J Clin. 2023;73(1):17–48. doi: 10.3322/caac.21763. PMID: 36633525. (2023).
- Karasaki, T. et al. Evolutionary characterization of lung adenocarcinoma morphology in TRACERx. *Nat. Med.* **29** (4), 833–845. <https://doi.org/10.1038/s41591-023-02230-w> (2023). Epub 2023 Apr 12. PMID: 37045996; PMCID: PMC7614478.
- Gillette, M. A. et al. Clinical Proteomic Tumor Analysis Consortium. Proteogenomic characterization reveals therapeutic vulnerabilities in Lung Adenocarcinoma. *Cell* **182** (1), 200–225e35. <https://doi.org/10.1016/j.cell.2020.06.013> (2020). PMID: 32649874; PMCID: PMC7373300.
- Yang, R. et al. The NLRP11 protein bridges the histone lysine acetyltransferase KAT7 to Acetylate Vimentin in the early stage of lung adenocarcinoma. *Adv. Sci. (Weinh.)* **10** (25), e2300971. <https://doi.org/10.1002/adv.202300971> (2023). Epub 2023 Jul 9. PMID: 37424170; PMCID: PMC10477884.
- Wilson, D. M. 3 et al. Hex1: a new human Rad2 nuclease family member with homology to yeast exonuclease 1. *Nucleic Acids Res.* **26** (16), 3762–3768. <https://doi.org/10.1093/nar/26.16.3762> (1998). PMID: 9685493; PMCID: PMC147753.
- Lee, B. I. & Wilson, D. M. 3rd. The RAD2 domain of human exonuclease 1 exhibits 5' to 3' exonuclease and flap structure-specific endonuclease activities. *J Biol Chem.* **274**(53):37763–9. (1999). <https://doi.org/10.1074/jbc.274.53.37763>. PMID: 10608837.
- Sertic, S., Quadri, R., Lazzaro, F. & Muzi-Falconi, M. EXO1: A tightly regulated nuclease. *DNA Repair (Amst.)* **93**:102929. (2020). <https://doi.org/10.1016/j.dnarep.2020.102929>. PMID: 33087266.
- Zhang, M., Zhao, D., Yan, C., Zhang, L. & Liang, C. Associations between nine polymorphisms in EXO1 and Cancer susceptibility: a systematic review and Meta-analysis of 39 case-control studies. *Sci. Rep.* **6**, 29270. <https://doi.org/10.1038/srep29270> (2016). PMID: 27387683; PMCID: PMC4937237.
- Michailidou, K. et al. Genome-wide association analysis of more than 120,000 individuals identifies 15 new susceptibility loci for breast cancer. *Nat. Genet.* **47** (4), 373–380. <https://doi.org/10.1038/ng.3242> (2015). Epub 2015 Mar 9. PMID: 25751625; PMCID: PMC4549775.
- Ren, Q. et al. A novel signature predicts prognosis and immunotherapy in lung adenocarcinoma based on cancer-associated fibroblasts. *Front. Immunol.* **14**, 1201573. <https://doi.org/10.3389/fimmu.2023.1201573> (2023). PMID: 37325647; PMCID: PMC10264584.
- Ma, J. et al. Exonuclease 1 is a potential Diagnostic and Prognostic Biomarker in Hepatocellular Carcinoma. *Front. Mol. Biosci.* **9**, 889414. <https://doi.org/10.3389/fmolb.2022.889414> (2022). PMID: 35769911; PMCID: PMC9234278.
- Yang, G. et al. EXO1 plays a carcinogenic role in Hepatocellular Carcinoma and is related to the regulation of FOXP3. *J. Cancer.* **11** (16), 4917–4932. <https://doi.org/10.7150/jca.40673> (2020). PMID: 32626539; PMCID: PMC7330697.
- Wang, Z. et al. EXO1/P53/SREBP1 axis-regulated lipid metabolism promotes prostate cancer progression. *J. Transl Med.* **22** (1), 104. <https://doi.org/10.1186/s12967-023-04822-z> (2024). PMID: 38279172; PMCID: PMC10811948.
- Liu, J. & Zhang, J. Elevated EXO1 expression is associated with breast carcinogenesis and poor prognosis. *Ann. Transl Med.* **9** (2), 135. <https://doi.org/10.21037/atm-20-7922> (2021). PMID: 33569437; PMCID: PMC7867906.
- Yuan, R. et al. The roles of tissue-Resident memory T cells in Lung diseases. *Front. Immunol.* **12**, 710375. <https://doi.org/10.3389/fimmu.2021.710375> (2021). PMID: 34707601; PMCID: PMC8542931.
- Mueller, S. N. & Mackay, L. K. Tissue-resident memory T cells: local specialists in immune defence. *Nat. Rev. Immunol.* **16** (2), 79–89. <https://doi.org/10.1038/nri.2015.3> (2016). Epub 2015 Dec 21. PMID: 26688350.
- Clark, R. A. Resident memory T cells in human health and disease. *Sci. Transl Med.* **7** (269), 269rv1. <https://doi.org/10.1126/scitranslmed.3010641> (2015). PMID: 25568072; PMCID: PMC4425129.
- Schenkel, J. M. & Masopust, D. Tissue-resident memory T cells. *Immunity* **41** (6), 886–897. <https://doi.org/10.1016/j.immuni.2014.12.007> (2014). Epub 2014 Dec 6. PMID: 25526304; PMCID: PMC4276131.
- Snyder, M. E. & Farber, D. L. Human lung tissue resident memory T cells in health and disease. *Curr. Opin. Immunol.* **59**, 101–108. <https://doi.org/10.1016/j.coi.2019.05.011> (2019). Epub 2019 Jun 29. PMID: 31265968; PMCID: PMC6774897.
- Byrne, A. et al. Tissue-resident memory T cells in breast cancer control and immunotherapy responses. *Nat. Rev. Clin. Oncol.* **17** (6), 341–348. <https://doi.org/10.1038/s41571-020-0333-y> (2020). Epub 2020 Feb 28. PMID: 32112054.
- Noble, A. et al. Altered immunity to microbiota, B cell activation and depleted  $\gamma\delta$ /resident memory T cells in colorectal cancer. *Cancer Immunol. Immunother.* **71** (11), 2619–2629. <https://doi.org/10.1007/s00262-021-03135-8> (2022). Epub 2022 Mar 22. PMID: 35316367; PMCID: PMC9519644.
- Webb, J. R., Milne, K., Watson, P., Deleew, R. J. & Nelson, B. H. Tumor-infiltrating lymphocytes expressing the tissue resident memory marker CD103 are associated with increased survival in high-grade serous ovarian cancer. *Clin Cancer Res.* **20**(2):434–44. (2014). <https://doi.org/10.1158/1078-0432.CCR-13-1877>. Epub 2013 Nov 4. PMID: 24190978.
- Edwards, J. et al. CD103+ tumor-resident CD8+ T cells are Associated with Improved Survival in Immunotherapy-Naïve Melanoma patients and Expand significantly during Anti-PD-1 treatment. *Clin. Cancer Res.* **24** (13), 3036–3045. <https://doi.org/10.1158/1078-0432.CCR-17-2257> (2018). Epub 2018 Mar 29. PMID: 29599411.
- Amsen, D., van Gisbergen, K. P. J. M., Hombrink, P. & van Lier, R. A. W. Tissue-resident memory T cells at the center of immunity to solid tumors. *Nat. Immunol.* **19** (6), 538–546. <https://doi.org/10.1038/s41590-018-0114-2> (2018). Epub 2018 May 18. PMID: 29777219.
- Poon, M. M. L. et al. Tissue adaptation and clonal segregation of human memory T cells in barrier sites. *Nat. Immunol.* **24** (2), 309–319. <https://doi.org/10.1038/s41590-022-01395-9> (2023). Epub 2023 Jan 19. PMID: 36658238; PMCID: PMC10063339.
- Hu, F. F., Liu, C. J., Liu, L. L., Zhang, Q. & Guo, A. Y. Expression profile of immune checkpoint genes and their roles in predicting immunotherapy response. *Brief Bioinform.* **22**(3):bbaa176. (2021). <https://doi.org/10.1093/bib/bbaa176>. PMID: 32814346.
- Lu, Y. et al. The FBXO32/ATR/ATM axis acts as a molecular switch to control the sensitivity of osteosarcoma cells to irradiation through its regulation of EXO1 expression. *Acta Biochim. Biophys. Sin. (Shanghai)* **55** (5), 842–852. <https://doi.org/10.3724/abbs.2023049> (2023). PMID: 37227155; PMCID: PMC10281878.
- Tomimatsu, N. et al. Phosphorylation of EXO1 by CDKs 1 and 2 regulates DNA end resection and repair pathway choice. *Nat. Commun.* **5**, 3561. <https://doi.org/10.1038/ncomms4561> (2014). PMID: 24705021; PMCID: PMC4041212.
- Bologna, S. et al. Sumoylation regulates EXO1 stability and processing of DNA damage. *Cell. Cycle.* **14** (15), 2439–2450. <https://doi.org/10.1080/15384101.2015.1060381> (2015). Epub 2015 Jun 17. PMID: 26083678; PMCID: PMC4615030.

30. Erdal, E., Haider, S., Rehwinkel, J., Harris, A. L. & McHugh, P. J. A prosurvival DNA damage-induced cytoplasmic interferon response is mediated by end resection factors and is limited by Trex1. *Genes Dev.* **31** (4), 353–369. <https://doi.org/10.1101/gad.289769.116> (2017). Epub 2017 Mar 9. PMID: 28279982; PMCID: PMC5358756.
31. Desai, A., Webb, B. & Gerson, S. L. CD133+ cells contribute to radioresistance via altered regulation of DNA repair genes in human lung cancer cells. *Radiother Oncol.* **110** (3), 538–545. <https://doi.org/10.1016/j.radonc.2013.10.040> (2014). Epub 2014 Jan 16. PMID: 24440048; PMCID: PMC4004669.
32. Gao, Y. et al. DNA repair gene polymorphisms and tobacco smoking in the risk for colorectal adenomas. *Carcinogenesis* **32** (6), 882–887. <https://doi.org/10.1093/carcin/bgr071> (2011). Epub 2011 Apr 18. PMID: 21504893; PMCID: PMC3106441.
33. Keijzers, G. et al. Human exonuclease 1 (EXO1) Regulatory functions in DNA replication with putative roles in Cancer. *Int. J. Mol. Sci.* **20** (1), 74. <https://doi.org/10.3390/ijms20010074> (2018). PMID: 30585186; PMCID: PMC6337416.
34. Kanehisa, M. & Goto, S. KEGG: kyoto encyclopedia of genes and genomes. *Nucleic Acids Res.* **28** (1), 27–30. <https://doi.org/10.1093/nar/28.1.27> (2000). PMID: 10592173; PMCID: PMC102409.
35. Fan, J. et al. Phospholipase C-ε regulates bladder cancer cells via ATM/EXO1. *Am. J. Cancer Res.* **10** (8), 2319–2336 (2020). PMID: 32905533; PMCID: PMC7471350.
36. Ireland, A. S. et al. MYC drives temporal evolution of small cell Lung Cancer subtypes by reprogramming neuroendocrine fate. *Cancer Cell.* **38** (1), 60–78e12. <https://doi.org/10.1016/j.ccell.2020.05.001> (2020). Epub 2020 May 30. PMID: 32473656; PMCID: PMC7393942.
37. Shih, D. J. H. et al. Genomic characterization of human brain metastases identifies drivers of metastatic lung adenocarcinoma. *Nat. Genet.* **52** (4), 371–377. <https://doi.org/10.1038/s41588-020-0592-7> (2020). Epub 2020 Mar 23. PMID: 32203465; PMCID: PMC7136154.
38. Kortlever, R. M. et al. Myc cooperates with Ras by programming inflammation and Immune suppression. *Cell* **171** (6), 1301–1315e14 (2017). PMID: 29195074; PMCID: PMC5720393.
39. Yin, X. et al. Small cell lung cancer transformation: from pathogenesis to treatment. *Semin Cancer Biol.* **86** (Pt 2), 595–606 (2022). Epub 2022 Mar 8. PMID: 35276343.
40. Marcoux, N. et al. EGFR-Mutant Adenocarcinomas that transform to small-cell Lung Cancer and other neuroendocrine carcinomas: clinical outcomes. *J. Clin. Oncol.* **37** (4), 278–285. <https://doi.org/10.1200/JCO.2018.01585> (2019). Epub 2018 Dec 14. PMID: 30550363; PMCID: PMC7001776.
41. Guan, J. et al. MLH1 Deficiency-Triggered DNA Hyperexcision by Exonuclease 1 Activates the cGAS-STING Pathway. *Cancer Cell.* **39**(1):109–121.e5. (2021). <https://doi.org/10.1016/j.ccell.2020.11.004>. Epub 2020 Dec 17. PMID: 3338427; PMCID: PMC8666006.
42. Pitt, J. M. et al. Targeting the tumor microenvironment: removing obstruction to anticancer immune responses and immunotherapy. *Ann. Oncol.* **27** (8), 1482–1492. <https://doi.org/10.1093/annonc/mdw168> (2016). Epub 2016 Apr 10. PMID: 27069014.
43. Bejarano, L., Jordão, M. J. C. & Joyce, J. A. Therapeutic Targeting of the Tumor Microenvironment. *Cancer Discov.* **11**(4):933–959. (2021). <https://doi.org/10.1158/2159-8290.CD-20-1808>. PMID: 33811125.
44. Djenidi, F. et al. CD8 + CD103 + tumor-infiltrating lymphocytes are tumor-specific tissue-resident memory T cells and a prognostic factor for survival in lung cancer patients. *J. Immunol.* **194** (7), 3475–3486. <https://doi.org/10.4049/jimmunol.1402711> (2015). Epub 2015 Feb 27. PMID: 25725111.
45. Ganesan, A. P. et al. Tissue-resident memory features are linked to the magnitude of cytotoxic T cell responses in human lung cancer. *Nat. Immunol.* **18** (8), 940–950. <https://doi.org/10.1038/ni.3775> (2017). Epub 2017 Jun 19. PMID: 28628092; PMCID: PMC6036910.
46. Oja, A. E. et al. Functional heterogeneity of CD4+ tumor-infiltrating lymphocytes with a Resident Memory phenotype in NSCLC. *Front. Immunol.* **9**, 2654. <https://doi.org/10.3389/fimmu.2018.02654> (2018). PMID: 30505306; PMCID: PMC6250821.
47. Clarke, J. et al. Single-cell transcriptomic analysis of tissue-resident memory T cells in human lung cancer. *J. Exp. Med.* **216** (9), 2128–2149. <https://doi.org/10.1084/jem.20190249> (2019). Epub 2019 Jun 21. PMID: 31227543; PMCID: PMC6719422.
48. Weeden, C. E. et al. Early immune pressure initiated by tissue-resident memory T cells sculpts tumor evolution in non-small cell lung cancer. *Cancer Cell.* **41** (5), 837–852e6 (2023). Epub 2023 Apr 21. PMID: 37086716.
49. Savas, P. et al. Single-cell profiling of breast cancer T cells reveals a tissue-resident memory subset associated with improved prognosis. *Nat. Med.* **24**(7):986–993. (2018). <https://doi.org/10.1038/s41591-018-0078-7>. Epub 2018 Jun 25. Erratum in: *Nat. Med.* **2018**;24(12):1941. doi: 10.1038/s41591-018-0176-6. PMID: 29942092.
50. Brewitz, A. et al. CD8+ T cells orchestrate pDC-XCR1+ dendritic cell spatial and functional cooperativity to optimize priming. *Immunity* **46** (2), 205–219. <https://doi.org/10.1016/j.immuni.2017.01.003> (2017). Epub 2017 Feb 9. PMID: 28190711; PMCID: PMC5362251.
51. Cunnea, P. et al. Spatial and temporal intra-tumoral heterogeneity in advanced HGSOc: implications for surgical and clinical outcomes. *Cell. Rep. Med.* **4** (6), 101055. <https://doi.org/10.1016/j.xcrm.2023.101055> (2023). Epub 2023 May 22. PMID: 37220750; PMCID: PMC10313917.
52. Zhou, K. I. et al. Spatial and temporal heterogeneity of PD-L1 expression and Tumor Mutational Burden in Gastroesophageal Adenocarcinoma at Baseline diagnosis and after Chemotherapy. *Clin. Cancer Res.* **26** (24), 6453–6463. <https://doi.org/10.1158/1078-0432.CCR-20-2085> (2020). Epub 2020 Aug 20. PMID: 32820017; PMCID: PMC7744325.
53. Mantovani, A., Marchesi, F., Malesci, A., Laghi, L. & Allavena, P. Tumour-associated macrophages as treatment targets in oncology. *Nat. Rev. Clin. Oncol.* **14** (7), 399–416. <https://doi.org/10.1038/nrclinonc.2016.217> (2017). Epub 2017 Jan 24. PMID: 28117416; PMCID: PMC5480600.
54. Mantovani, A., Allavena, P., Marchesi, F. & Garlanda, C. Macrophages as tools and targets in cancer therapy. *Nat. Rev. Drug Discov.* **21** (11), 799–820. <https://doi.org/10.1038/s41573-022-00520-5> (2022). Epub 2022 Aug 16. PMID: 35974096; PMCID: PMC9380983.
55. Li, Z. et al. Comprehensive analyses for the coagulation and macrophage-related genes to reveal their joint roles in the prognosis and immunotherapy of lung adenocarcinoma patients. *Front. Immunol.* **14**, 1273422. <https://doi.org/10.3389/fimmu.2023.1273422> (2023). PMID: 38022584; PMCID: PMC10644034.
56. Garrido-Martin, E. M. et al. M1<sup>hot</sup> tumor-associated macrophages boost tissue-resident memory T cells infiltration and survival in human lung cancer. *J. Immunother. Cancer.* **8** (2), e000778. <https://doi.org/10.1136/jitc-2020-000778> (2020). PMID: 32699181; PMCID: PMC7375465.

## Acknowledgements

We are very grateful to Gene-Expression Omnibus (GEO) and the Cancer Genome Atlas (TCGA) databases for providing the transcriptome and clinical information.

## Author contributions

L.Z. and X.L. were responsible for data acquisition, partial data analysis and drafted the original manuscript. Y.Y. performed immunohistochemical staining for the clinical tissue and related data analysis. M.T., L.Z., F.H. and X.W. were responsible for manuscript editing and data corrections. Y.T. and Z.W. conceived the idea, designed this study and reviewed the original manuscript. All authors read and approved the final version of the manu-

script.

### Funding

The study was funded by Clinical Research Fund of Shandong Medical Association Qilu Special Project (YX-H2022ZX02016; Yuan Tian) and Clinical Research Special Support Fund of Wu Jieping Medical Foundation (320.6750.2023-16-12; Yuan Tian).

### Declarations

#### Conflict of interest

The authors declare no conflicts of interest.

#### Ethics approval

The study was conducted in accordance with the Declaration of Helsinki, and approved by the Ethics Committee of Shandong Provincial Hospital (protocol code SWYX2024-394 and date of approval is July 26th, 2024). Informed consent was obtained from all of the subjects or their legal guardians.

#### Additional information

**Supplementary Information** The online version contains supplementary material available at <https://doi.org/10.1038/s41598-025-88126-w>.

**Correspondence** and requests for materials should be addressed to Z.W. or Y.T.

**Reprints and permissions information** is available at [www.nature.com/reprints](http://www.nature.com/reprints).

**Publisher's note** Springer Nature remains neutral with regard to jurisdictional claims in published maps and institutional affiliations.

**Open Access** This article is licensed under a Creative Commons Attribution-NonCommercial-NoDerivatives 4.0 International License, which permits any non-commercial use, sharing, distribution and reproduction in any medium or format, as long as you give appropriate credit to the original author(s) and the source, provide a link to the Creative Commons licence, and indicate if you modified the licensed material. You do not have permission under this licence to share adapted material derived from this article or parts of it. The images or other third party material in this article are included in the article's Creative Commons licence, unless indicated otherwise in a credit line to the material. If material is not included in the article's Creative Commons licence and your intended use is not permitted by statutory regulation or exceeds the permitted use, you will need to obtain permission directly from the copyright holder. To view a copy of this licence, visit <http://creativecommons.org/licenses/by-nc-nd/4.0/>.

© The Author(s) 2025